Microwave-assisted extraction of rare earth elements from petroleum refining catalysts and ambient fine aerosols prior to inductively coupled plasma-mass spectrometry

ARTICLE *in* ANALYTICA CHIMICA ACTA · FEBRUARY 2007

Impact Factor: 4.51 · DOI: 10.1016/j.aca.2006.08.035 · Source: PubMed

3 AUTHORS, INCLUDING:

Shankar Chellam
Texas A&M University
107 PUBLICATIONS **2,317** CITATIONS
SEE PROFILE

David W. Mittlefehldt
NASA/Johnson Space Center
419 PUBLICATIONS **6,664** CITATIONS
SEE PROFILE

Available online at www.sciencedirect.com
ScienceDirect
Analytica Chimica Acta 581 (2007) 247–259
ANALYTICA CHIMICA ACTA
www.elsevier.com/locate/aca

Microwave-assisted extraction of rare earth elements from petroleum refining catalysts and ambient fine aerosols prior to inductively coupled plasma-mass spectrometry

Pranav Kulkarni [a], Shankararaman Chellam [a,b,*], David W. Mittlefehldt [c]

[a] *Department of Civil and Environmental Engineering, University of Houston, Houston, TX 77204-4003, United States*
[b] *Department of Chemical Engineering, University of Houston, Houston, TX 77204-4004, United States*
[c] *Astromaterials Research and Exploration Science Office, NASA Johnson Space Center, 2101 NASA Parkway, Houston, TX 77058, United States*

Received 25 May 2006; received in revised form 8 August 2006; accepted 16 August 2006
Available online 26 August 2006

Abstract

A robust microwave-assisted acid digestion procedure followed by inductively coupled plasma-mass spectrometry (ICP-MS) was developed to quantify rare earth elements (REEs) in fluidized-bed catalytic cracking (FCC) catalysts and atmospheric fine particulate matter ($PM_{2.5}$). High temperature (200 °C), high pressure (200 psig), acid digestion (HNO_3, HF and H_3BO_3) with 20 min dwell time effectively solubilized REEs from six fresh catalysts, a spent catalyst and $PM_{2.5}$. This method was also employed to measure 27 non-REEs including Na, Mg, Al, Si, K, Sc, Ti, V, Cr, Mn, Fe, Co, Ni, Cu, Zn, Ga, As, Se, Rb, Sr, Zr, Mo, Cd, Cs, Ba, Pb and U. Complete extraction of several REEs (Y, La, Ce, Pr, Nd, Tb, Dy and Er) required HF indicating that they were closely associated with the aluminosilicate structure of the zeolite FCC catalysts. Internal standardization using ^{115}In quantitatively corrected non-spectral interferences in the catalyst digestate matrix. Inter-laboratory comparison using ICP-optical emission spectroscopy (ICP-OES) and instrumental neutron activation analysis (INAA) demonstrated the applicability of the newly developed analytical method for accurate analysis of REEs in FCC catalysts. The method developed for FCC catalysts was also successfully implemented to measure trace to ultra-trace concentrations of La, Ce, Pr, Nd, Sm, Gd, Eu and Dy in ambient $PM_{2.5}$ in an industrial area of Houston, TX.

Keywords: Microwave digestion; Fluidized-bed catalytic cracking (FCC) catalysts; Inductively coupled plasma-mass spectrometry (ICP-MS); Instrumental neutron activation analysis (INAA); Rare earth elements; Lanthanides; Particulate matter ($PM_{2.5}$)

1. Introduction

Trace elements in $PM_{2.5}$ can serve as the basis of receptor-oriented modeling [1,2] and also provide important information for epidemiological studies. To date, the vast majority of studies on trace elements in ambient aerosols have only focused on the main groups and main transition series (d-block) elements, e.g. [3–8]. Only a very select number of studies have focused on rare earth elements (REEs), e.g. [9,10], which comprise the elements Y, La, and the lanthanides (Ce–Lu) [11].

It is crucial to monitor REEs in $PM_{2.5}$, especially in industrial environments, because they are excellent tracers to track fluidized-bed catalytic cracking (FCC) emissions from petroleum refining operations [9,10,12]. Even though La and Ce have been reported for vehicle $PM_{2.5}$ emissions [13,14] and occasionally in ambient PM [3,8], analyzing other lanthanides is essential to identify loss of FCC catalysts from petroleum refineries and their contributions to ambient $PM_{2.5}$.

A major challenge in quantifying REEs emissions from refineries is the lack of a certified reference material for FCC catalysts [15]. Additionally, because REEs are present only in trace to ultra-trace levels in ambient $PM_{2.5}$ they are difficult to measure accurately and precisely, necessitating either high temperature–high pressure microwave assisted acid ($HNO_3 + HF + H_3BO_3$) digestion followed by inductively coupled plasma-mass spectrometry (ICP-MS) [4,8] or instrumental

* Corresponding author at: Department of Civil and Environmental Engineering, University of Houston, 4800 Calhoun Road, Houston, TX 77204-4003, United States. Tel.: +1 713 743 4265; fax: +1 713 743 4260.
E-mail address: chellam@uh.edu (S. Chellam).

0003-2670/$ – see front matter © 2006 Elsevier B.V. All rights reserved.
doi:10.1016/j.aca.2006.08.035

neutron activation analysis (INAA) [12]. Even though INAA is a non-destructive technique that can accurately quantify selected REEs: (1) it cannot quantify all REEs, (2) has a long time-lag between start of the experiment and final data compilation, (3) requires a high level of infrastructure (e.g. irradiation facility) and (4) produces low-level nuclear waste that remains radioactive for decades. In contrast, accurate and precise trace-level analysis of several elements including REEs at high throughput, relatively low cost, and creating less waste disposal issues can be achieved using microwave digestion followed by ICP-MS. One advantage of INAA is that minimal sample preparation is required – grinding, homogenizing and splitting – and this makes the technique ideal for validation of methods that require more elaborate sample processing such as ICP-MS.

To date, REEs have been quantified in natural biological, industrial, and geological samples, such as peat, plant, soil, sediment, tissue, meteorites, ores, etc. [16–23]. In contrast, FCC catalysts are anthropogenic, which are manufactured by incorporating REE cations in a zeolite support, and contain higher levels of siliceous matter. Therefore, previously developed methods cannot be directly applied to them because of matrix-induced complications and difficulties in solubilizing the aluminosilicate backbone of zeolites.

The principal objective of this research is to develop a robust method for accurate and precise quantitation of all naturally occurring REEs (Y, La, Ce, Pr, Nd, Sm, Eu, Gd, Tb, Dy, Ho, Er, Tm, Yb and Lu) present in FCC catalysts and ambient $PM_{2.5}$. Twenty-seven other elements (Na, Mg, Al, Si, K, Sc, Ti, V, Cr, Mn, Fe, Co, Ni, Cu, Zn, Ga, As, Se, Rb, Sr, Zr, Mo, Cd, Cs, Ba, Pb and U) were also measured. A combination of HNO_3, HF, and H_3BO_3 was employed to digest several representative catalysts (six fresh and one spent) and $PM_{2.5}$ in a microwave oven followed by ICP-MS. The newly developed method was validated by independent analysis using inductively coupled plasma-optical emission spectrometry (ICP-OES) and INAA.

2. Experimental work

Because detailed information on catalysts and $PM_{2.5}$ sampling location and methods have been reported by us recently [10,24], only a brief summary is provided herein.

2.1. Catalysts

Six zeolite based fresh FCC catalysts (Grace Davison Inc., Columbia, MD) and a spent zeolite FCC catalyst was employed. Scanning electron micrographs of two representative fresh catalysts are given in Fig. 1a and b. Similar to other fresh catalysts, SMR1–SMR6 were spherical having smooth surfaces [25]. Fig. 1c shows that in contrast to the fresh catalysts, the spent catalyst's surface was nodular and rough, caused by chemical contamination and abrasion. Substantial differences in the morphology between the fresh and spent catalysts demonstrate the need to include both types for development of a robust analytical method that will be applicable to all FCC zeolite catalysts. All samples were dried at 80 °C for 4 h in a clean oven and stored in a desiccator before use.

2.2. Ambient fine particles

Twenty-five $PM_{2.5}$ samples were collected from the HRM3 monitoring station (1504 1/2 Haden Road, Houston, TX 77015; latitude: 29.76527, longitude: −95.18101) located in an industrial park surrounded by numerous petroleum refineries in the Houston Ship Channel area [10,24].

One additional ambient $PM_{2.5}$ sample was also collected during an "increased air emissions event" from a $PM_{2.5}$ monitoring site "Kingwood C309" (3603 1/2 West Lake Houston Parkway, Houston, TX 77339; latitude: 30.05833, longitude: −95.18972) located near a residential area on 3 September 2005. Based on the information given by the Texas Commission on Environmental Quality (TCEQ), the increased air emissions event was caused by a malfunctioning wet gas compressor in a local oil refinery, releasing an estimated 26 kg PM, 376 kg CO, 137 kg NO, 1231 kg SO_2, and 1304 kg volatile organic compounds into the atmosphere. During this episode, the air quality in the vicinity of the refinery exceeded the Federal limit (National Ambient Air Quality Standard) and was categorized as 'unhealthy' by the TCEQ. This increase in fine particles is depicted in Fig. 2, which shows hourly $PM_{2.5}$ concentrations data captured at another monitoring site "C15/A115" (1405 Sheldon Road, Houston, TX 77530; latitude: 29.80250, longitude: −95.12556) which is in the close vicinity of the responsible local refinery.

2.3. Reagents and standards

65% HNO_3 and 99.99% H_3BO_3 (Suprapurgrade, EM Science, Gibbstown, NJ), 48% HF (PPB/Teflon grade, Fluka, Milwaukee, WI) were employed for sample digestions. REE preconcentrations [26,27] prior to ICP-OES analyses (see Section 2.8) were performed using *n*-heptane (AR grade, Fluka,

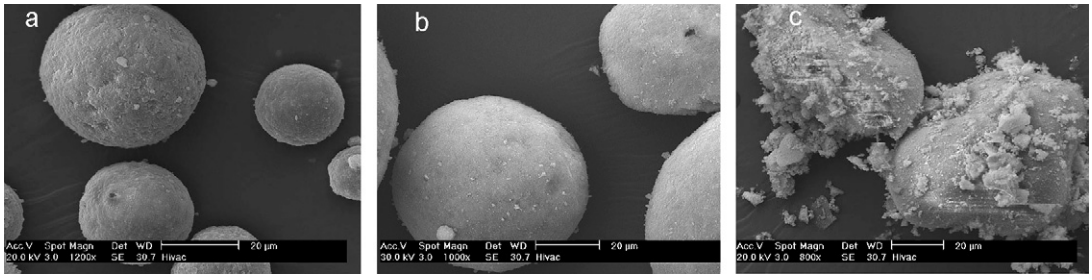

Fig. 1. SEM images of typical fresh catalysts SMR1 and SMR2 ((a) and (b), respectively) and spent catalyst (c).

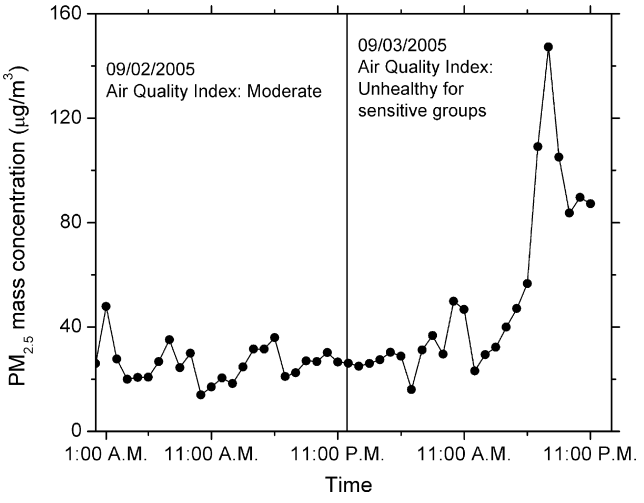

Fig. 2. Hourly $PM_{2.5}$ concentrations during an increased air emission event at site "C15/A115" in the Houston Ship Channel area on 2 and 3 September 2005, provided by the Texas Commission on Environmental Quality.

Milwaukee, WI), *n*-octanol (99+% HPLC Grade Fluka, Milwaukee, WI), diester mix of 65% bis(2-ethylhexyl) hydrogen phosphate and 35% 2-ethylhexyl dihydrogen phosphate (Tokyo Kasei Co. Ltd., Portland, OR).

Ultra-high purity water from a commercial system (Max159 Modulab, US Filter Corporation, Lowell, MA) was used for all solution preparations and dilutions. Multi-element ICP-MS and ICP-OES calibration solutions were prepared using 1 mg L^{-1} working standard solutions obtained by mixing 10 mg L^{-1} single element standards (High Purity Standards, Charleston, SC). The composition of the background solution used for reagent blanks, internal standards, and calibration was kept identical to the final digestate (see Section 2.4) in order to avoid errors related to matrix inconsistencies. Two working standards were prepared, one containing 15 REEs (Pm cannot be analyzed because it has no naturally occurring stable isotope [11]) and another containing the 27 non-REEs. To correct for instrumental drift and plasma fluctuations, all solutions were spiked with an internal standard (5 μg L^{-1} ^{115}In) prior to ICP-MS and ICP-OES analysis. Storage of standards and reagents and labware cleaning procedures has been described elsewhere by us [4].

2.4. Closed vessel acid digestion

Digestions were performed in a programmable 1200 W microwave (MARS 5, CEM Corp., Matthews, NC) using 100 mL Teflon-lined vessels rated at 210 °C and 350 psig (HP-500 Plus, CEM Corp., Matthews, NC). Pressure and temperature profiles in the vessels were digitally acquired at a frequency of 1/3 Hz during the heating and cooling cycles on an external computer to better evaluate the effects of experimental variables on sample digestion.

The effect of HF volume on digestion was evaluated for all the catalysts using a fixed volume (5 mL) of HNO_3. Fifty milligram of each catalyst were aliquoted into six separate Teflon vessels and varying the volume of HF in each vessel (0.00, 0.05, 0.10, 0.30, 0.50 or 1.00 mL). The vessels were capped, placed in the microwave system, and digested using a two-stage procedure. In the first stage, the temperature was ramped to 200 °C with the application of 600 W power followed by a dwell time of 20 min. Only for the case of 0.3 mL HF, lower temperature settings of 150 and 175 °C were also evaluated. The vessels were allowed to cool for 60–90 min, and then vented and opened.

In the second stage, remaining HF was complexed by adding stoichiometric excess of H_3BO_3 (5% (m/v) solution corresponding to eight times the HF volume) because several elements including REEs and few alkaline earth elements form insoluble fluoride precipitates leading to insufficient recovery. (Not incorporating H_3BO_3 after using HF may result in REE concentrations below ICP-MS method detection limits, e.g. [8].) The vessels were recapped and heated again to set points of 200 °C, 200 psig, with 20 min dwell time. After cooling, a 4.29 mL aliquot of the digestate was first diluted to 2% HNO_3 concentration using ultrapure water and further diluted 10-, 100- or 1000-fold as necessary to bring all analytes within the ICP-MS and ICP-OES dynamic range.

Ambient $PM_{2.5}$ filters were also digested using the same two-stage technique determined to be optimal for FCC catalysts (200 °C, 200 psig and 20 min dwell time). Acid volumes were proportionately reduced for these measurements since total $PM_{2.5}$ mass on each of the filters was only in the range of 0.2–0.5 mg. Additional discussion of acid volumes used to digest ambient $PM_{2.5}$ is given in Section 3.5. H_2O_2 addition [4,5,7] was not necessary because a clear solution was obtained with HNO_3, HF, and H_3BO_3 alone.

2.5. ICP-MS

The ICP-MS (Elan 6000, Perkin-Elmer, Norwalk, CT) was tuned using a solution of 10 μg L^{-1} of Ba, Cd, Ce, Cu, Ge, Mg, Pb, Rh, Sc, Tb, and Tl in 2% HNO_3 to verify mass resolution. This was followed by X–Y adjustment, argon gas flow and lens optimization, and an instrument performance check. Nebulizer and auxiliary gas flows were separately adjusted along with the torch position to minimize Ce and Ba oxide formation rates and maximize ^{103}Rh count rates. The mass spectrometer was calibrated separately using two external standards solutions, one consisting of 15 REEs and the other having 27 non-REEs. The final digestate after appropriate dilution and the internal standard solution (5 μg L^{-1} ^{115}In) were mixed prior to nebulization. The instrument was calibrated separately for REEs and non-REEs, which were then analyzed in two different runs. Platinum cones were cleaned periodically in a 2% HNO_3 solution by ultrasonication for 2 min at room temperature. Instrumental operating parameters are summarized in Table 1.

2.6. ICP-OES

An ICP-OES (4300 DV Perkin-Elmer instruments, Shelton, CT) housed in another laboratory located at Rice University, Houston, TX was used to compare ICP-MS results obtained for each catalyst sample. The same blanks, multi-element external standards, and internal standard solutions used for ICP-MS were also used with the ICP-OES. Operating conditions and spectral

Table 1
Operating conditions and instrumental setup for ICP-MS and ICP-OES

	ICP-MS	ICP-OES
Instrument	Elan 6000 (Perkin-Elmer, Norwalk, CT, USA), Gem-Tip crossflow nebulizer, Ryton spray chamber, four-channel peristaltic pump (Gibson, Model Minipuls III)	Perkin-Elmer 4300 DV, SCD detector, cyclonic spray chamber, Gem-Tip cross flow nebulizer
RF power	1300 W	1150 W
Nebulizer gas flow	0.85–1.00 L min^{-1} optimized for each analysis to maximize the counts and minimize the oxide formation	0.85 L min^{-1}
Auxiliary gas flow	0.8 L min^{-1}	0.8 L min^{-1}
Lens voltage	6.5 V	Not applicable
Cones	Pt sampler (1.1 mm orifice i.d.), Pt skimmer (0.8 mm orifice i.d.)	Not applicable
Sampling parameters	AS-90, Perkin-Elmer autosampler, sample uptake rate 1 mL min^{-1}, rinsing time 60 s (2% HNO_3), signal read delay time 35 s	AS-93 plus, Perkin-Elmer autosampler, sample uptake rate 1.5 mL min^{-1}, rinsing time 60 s (2% HNO_3)
Data acquisition	Peak hopping mode, 50 sweeps per reading, 3 readings per replicate, 3 replicates, dwell time 100 ms	3 reading per replicate, 3 replicates, wavelengths: La (398.852 nm), Ce (413.764 nm), Pr (390.844 nm), Dy (353.170 nm), Er (337.271 nm), Eu (381.967 nm), Gd (342.247 nm), Ho (345.600 nm), Nd (406.109 nm), Sm (359.260 nm), Tb (350.917 nm), Yb (328.937 nm), Tm (313.126 nm), Lu (261.542 nm), Y (371.029 nm)
Time	3–4 min per sample	2–3 min per sample

lines used for REE analysis are also listed in Table 1. Operating parameters especially, nebulizer gas flow and the ICP generator power were all optimized to minimize spectral overlaps of the blank corrected emission intensities for all 42 elements monitored herein.

2.7. INAA

Instrumental neutron activation analysis was performed in the Gamma-ray Spectroscopy Laboratory (GSL) of NASA/Johnson Space Center, Houston, TX. Catalyst samples, standards, and controls (see Section 2.9) were first irradiatiated for 2 h in a irradiation can at a thermal neutron flux of 6.6×10^{12} n cm^{-2} s^{-1} at Texas A&M University Nuclear Science Center, College Station, TX and then the irradiation can was shipped overnight to GSL, Houston, TX. Because FCC catalysts contained 10^3 to 10^6 times the light REE concentrations compared with the meteorite, lunar, and planetary samples normally analyzed in the GSL; they represented a serious potential contamination hazard for the laboratory and posed a significant analytical challenge. Hence, routine analysis procedures were modified to reduce neutron self-shielding (some REEs can have very high neutron capture cross sections) and mitigate the potential for laboratory contamination.

Plastic vials containing ∼2 g of each catalyst sample were shipped to GSL/NASA from which duplicate or triplicate splits, each ∼20 mg were analyzed. The samples were weighed into 0.3 mL polyethylene vials and heat sealed. Splits of ∼50 mg each of certified reference materials were similarly loaded and sealed. One sample of NIST 1633a coal fly ash was used as the primary standard for all elements except Na and Ca, for which International Working Group AN-G anorthosite was used as the standard.

For the first three count sets, samples and reference materials were counted in the GSL on two ∼15% efficiency intrinsic Ge detectors. Later counting was done using two ∼50% efficiency intrinsic Ge detectors in the low-level counting room. A series of four counts 2–3, 3–7, 16–21 and 36–47 days after irradiation were performed to acquire data on nuclides with differing half-lives listed in Table 2. Net peak areas were calculated from the raw spectral data using an updated version of the TEABAGS program [28]. Interference corrections, concentrations of elements, and initial data evaluation were carried out using additional in-house programs. Following automatic data reduction, the data were manually investigated and necessary background corrections and additional interference corrections were employed. INAA was used to quantify eight REEs (La, Ce, Nd, Sm, Eu, Tb, Yb and Lu) that could be precisely determined from the catalyst matrix and typically reported by others from other matrices, e.g. [12,16,36]. Four non-REEs (Na, Fe, Co and Ba) in FCC catalysts were also determined by INAA.

2.8. REE preconcentration

Tb, Ho, Tm, and Lu concentrations in final digestates were increased above ICP-OES detection limits by first extracting

Table 2
Nuclides for REEs utilized in INAA along with their half-lives and the specific photopeak energies used in the assay

Nuclide	^{140}La	^{141}Ce	^{147}Nd	^{153}Sm	^{152}Eu	^{160}Tb	^{169}Yb	^{175}Yb	^{177}Lu
Half-life (day)	1.68	32.6	11	1.95	4821	72.1	32	4.19	6.71
Gamma-ray energy (keV)	328.8, 487, 815.9, 1596.5	145.4	531	103.2	778.9, 1408.1	298.6	177.2	282.5, 396.3	208.3

them in 20 mL of a diester mix of 65% bis(2-ethylhexyl) hydrogen phosphate and 35% 2-ethylhexyl dihydrogen phosphate in *n*-heptane (P0261, Tokyo Kasei Co. Ltd.) [26,27]. REEs were back-extracted from the organic phase to the aqueous phase by adding 10 mL of octanol and 5 mL HCl. Traces of octanol were removed by washing the aqueous phase three times with 5 mL of *n*-heptane. The acid solution containing REEs was then evaporated to near dryness on a hot plate at 40 °C. Finally, the sample residues were dissolved in 4–10 mL of 2% HNO_3 prior to ICP-OES resulting in 10–25-fold enrichment for Tb, Ho, Tm and Lu.

2.9. Quality assurance

In the absence of a certified FCC catalyst reference material, several quality control and quality assurance measures were employed to stringently evaluate the newly developed analytical methods. First, a known concentration of each REE was spiked in aluminosilicate zeolite powder (ICN19390280, Fisher Scientific, Houston, TX) as well as each of the seven FCC catalysts and aged for 90 days. These spiked samples were digested using the optimal procedure and analyzed by ICP-MS to obtain REEs recoveries. Secondly, another catalyst type, SRM 2556 (recycled pellet automobile catalyst, NIST, Gaithersburg, MD) with specified amounts of La and Ce was also used to ensure the validity of our ICP-MS methods. Thirdly, we compared REE concentrations obtained from ICP-MS with ICP-OES and INAA.

A back-up sample of the primary standard was always included in the INAA procedure in case of failure during irradiation, plus one or more reference materials to act as quality controls. Splits of ~50 mg each of three certified reference materials (NIST 1633a coal fly ash, US Geological Survey BHVO-1 Hawaiian basalt, and International Working Group AN-G anorthosite) were used as controls. Thus, the second sample of NIST 1633a, the Na–Ca primary standard (AN-G) and BHVO-1 all provided checks on the accuracy of the INAA data.

Additionally, each digested $PM_{2.5}$ sample was analyzed in triplicate by ICP-MS along with a fourth replicate, to which known amounts of REEs were added to monitor matrix spike recoveries. Finally, $PM_{2.5}$ samples were collected intermittently over a 100-day period to potentially capture changes in meteorology and refinery operating conditions.

3. Results and discussion

3.1. Experimental reproducibility

Digestions and ICP-MS measurements were repeated on different dates during the course of our work using the newly developed optimal analytical method (see Section 3.5) for each of the catalysts. In all cases, no statistically significant differences ($p = 0.05$) in REE and non-REE concentrations was observed. Hence, each catalyst sample was homogenous and individual samples could be used separately for method development. Additionally, the coefficient of variation was always <10% demonstrating excellent precision in our measurements. These results demonstrate that all our digestion and ICP-MS

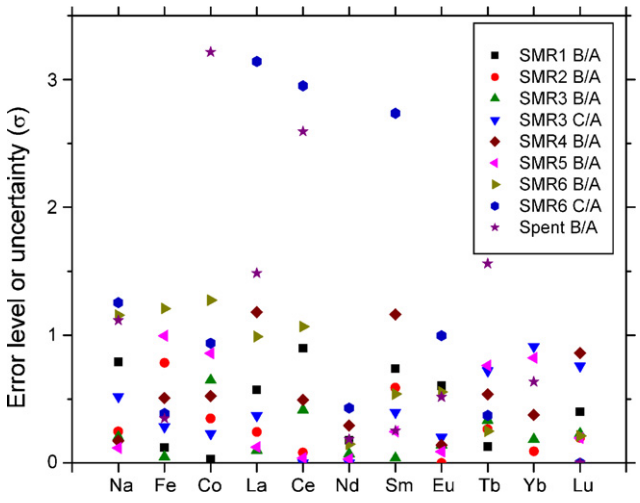

Fig. 3. Errors in INAA measurements within duplicate or triplicate (A, B and C) splits of individual zeolite catalysts.

experimental protocols were consistent and highly reproducible allowing a quantitative comparison of results generated over the entire duration of this study.

Standard statistical analyses were first performed on INAA measurements of elemental concentrations in the controls and reference materials to quantify its accuracy. The absolute departure of the INAA result from the recommended value was ratioed to the combined one standard deviation uncertainty, i.e. $|(X/R) - 1|/U$, where X was our determination, R is the recommended value (provided by NIST, USGS or the International Working Group), and U is the 1σ uncertainty in the ratio calculated from the 1σ INAA uncertainty and the 1σ confidence limit for the recommended value. For the elements analyzed, most determinations were within 1σ uncertainty and all but one was within 2σ uncertainty of the recommended values. Based on these results of analyses of controls, we conclude that the INAA analyses of unknowns samples (FCC catalysts) reported in this paper are accurate. Similar comparisons are depicted in Fig. 3 for the INAA results on different splits of individual catalyst samples. For the eight REEs and three non-REEs shown, determinations on replicate splits also agreed well statistically; of the 97 ratios calculated, 91 (94%) were within the 2σ (95%) limit indicating that the analyzed splits of each sample were representative and INAA provided reproducible measurements.

3.2. Temperature and pressure during microwave digestion

Microwave set points of 150 and 175 °C resulted in a black residue, demonstrating incomplete sample dissolution. Because a clear solution was obtained for 200 °C it was always selected as the set-point for future digestions.

Because temperature has a greater influence on solid sample dissolution than pressure [29], care was taken to ensure that it always remained the controlling parameter during microwave operation. Temperature and pressure profiles in the Teflon vessels for the optimal method are depicted in Fig. 4. As observed, the set-point of 200 °C was achieved with ~140 and 145 psig in the first and second stages, respectively. Higher pressures during

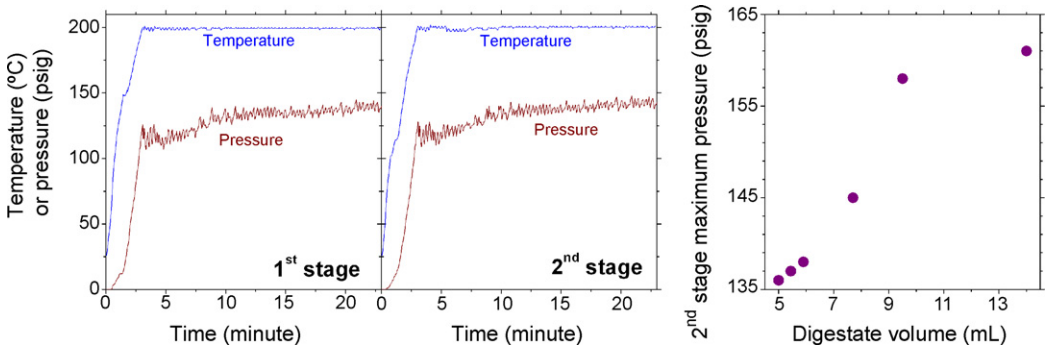

Fig. 4. Temperature and pressure profiles during two-stage digestion of 50 mg SMR1 with 5 mL HNO_3, 0.3 mL HF and 2.4 mL H_3BO_3 with set points of 200 °C and 200 psig and dwell time of 20 min (a and b). The maximum pressure reached in the second digestion stage as a function of total acid volume is also shown (c).

the second stage were caused by increased liquid volume due to H_3BO_3 addition.

Fig. 4c depicts the maximum pressure attained in the second stage with varying acid volumes for SMR1. Because first stage pressures remained ~140 psig even when different HF volumes were employed, it is not shown herein. The pressure in the extraction vessels can be seen to increase with digestate volume resulting from larger HF and H_3BO_3 additions, but never reached the 200 psig set-point. Hence, temperature controlled all the digestions resulting in reproducible and precise extractions. Similar results were obtained for all other catalysts and $PM_{2.5}$ where set point of 200 °C always yielded a colorless solution, indicating complete dissolution of the solid samples.

3.3. Mass spectral interferences and isotope selection

Potential interferences from polyatomic ions, isobaric overlaps, and relative abundances were all considered before selecting the most appropriate REE isotope for ICP-MS analysis. Depending on the plasma operating conditions, REEs can form oxides (MO^+) and hydroxides (MOH^+), which along with barium oxides can potentially cause severe spectral interferences [30]. Hence, nebulizer gas flow and RF power were carefully optimized by trial and error during instrument tuning to maximize the signal intensity (measured as ^{103}Rh counts) and minimize the oxide formation rates (measured as CeO/Ce counts), which was also frequently checked during analysis. Table 3 summarizes the REE isotopes chosen in this study for ICP-MS analysis along with their possible major interferences.

Even with the optimized instrumental conditions (Table 1), and maintaining $MO^+/M^+ < 5\%$ and $MOH^+/M^+ < 1.5\%$, Nd and Gd, which were present in high levels in FCC catalysts induced mass spectral overlaps (Table 3) resulting in significant systematic errors (15–45%) for Tb, Yb and Lu, which were present in much lower concentrations. (Note that using a high-resolution ICP-MS can largely eliminate this error. However, quadrupole based ICP-MS instruments, such as the one employed in this study are more common necessitating empirical interference correction equations for certain elements.) Therefore, matrix-induced polyatomic interferences for the monitored REE isotopes were corrected by obtaining oxide and hydroxide counts for single element solutions of Te, Ba, Ce, Nd, Gd, Sm, Pr, Eu and Tb prepared in the reagent blank solution. These elements were selected because they constitute the major REE interferences. Their concentrations were kept in the same range as that expected in catalyst samples. Intensities (I) for Nd, Sm, Eu, Gd, Tb, Er, Yb and Lu were mathematically corrected by applying correction equations, e.g.:

$$(I^{\text{corrected}}_{^{153}\text{Eu}})_{\text{sample}} = (I^{\text{measured}}_{^{153}\text{Eu}})_{\text{sample}} - (I^{\text{measured}}_{^{137}\text{Ba}})_{\text{sample}} \left(\frac{I^{\text{measured}}_{^{137}\text{Ba}^{16}\text{O}}}{I^{\text{measured}}_{^{137}\text{Ba}}} \right)_{\text{single element solution}}$$

3.4. Non-spectral interferences and internal standard selection

Non-spectral ICP-MS interferences for REEs arising from biological and environmental samples have been previously corrected using ^{102}Ru, ^{103}Rh, ^{115}In and ^{185}Re as internal standards [16,17,23]. However, FCC zeolite catalysts are predominantly composed of aluminosilicates (see Section 3.5) and the complete composition of their digestate matrix has not yet been established. Therefore, we evaluated several potential internal standards to accurately measure REEs.

HNO_3 solutions with concentrations of 0.0, 0.5, 1.0, 1.5 and 2.0%, each having 0.08% HF and 0.06% H_3BO_3 (identical to

Table 3
Isotopes selected for ICP-MS analysis along with their major potential spectral interferences in HNO_3–HF–H_3BO_3 matrix (adapted from [17])

Isotope	Abundance (%)	Main interferences
^{89}Y	100	$^{178}Hf^{++}$
^{139}La	99.91	$^{123}Sb^{16}O$
^{140}Ce	88.48	–
^{141}Pr	100	–
^{146}Nd	17.19	$^{130}Te^{16}O$
^{147}Sm	15	$^{130}Ba^{16}O^{1}H$
^{153}Eu	52.2	$^{137}Ba^{16}O$, $^{136}Ba^{16}O^{1}H$
^{158}Gd	24.84	$^{142}Nd^{16}O$
^{159}Tb	100	$^{143}Nd^{16}O$, $^{142}Nd^{16}O^{1}H$
^{163}Dy	24.9	$^{147}Sm^{16}O$
^{165}Ho	100	$^{149}Sm^{16}O$, $^{148}Nd^{16}O^{1}H$
^{166}Er	33.60	$^{150}Nd^{16}O$, $^{150}Sm^{16}O$
^{169}Tm	100	$^{153}Eu^{16}O$
^{172}Yb	21.9	$^{156}Gd^{16}O$
^{175}Lu	97.41	$^{159}Tb^{16}O$, $^{158}Gd^{16}O^{1}H$

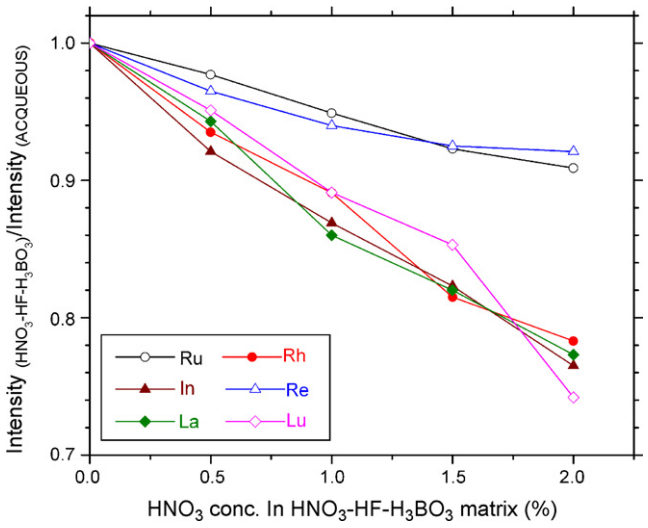

Fig. 5. Effect of HNO_3–HF–H_3BO_3 matrix on potential internal standards (^{102}Ru, ^{103}Rh, ^{115}In and ^{185}Re) along with a representative light REE (^{139}La) and a heavy REE (^{175}Lu). All intensities have been normalized by that corresponding to ultrapure water. Note that ultrapure water contained ultra-trace amount HNO_3 (<0.002%) due to the addition of REE containing standard solutions having 2% HNO_3.

the reagent blank) were spiked with all REEs in the similar concentration range as anticipated in the final catalyst digestate. Changes in REEs signal intensities in these solutions with varying HNO_3 concentrations were monitored along with each potential internal standard counts. Typical results obtained are depicted in Fig. 5 for one light (^{139}La) and one heavy (^{175}Lu) REE along with each of the four internal standards after normalizing intensities by that of the aqueous solution (0% HNO_3). Increasing HNO_3 concentrations suppressed signal intensities presumably due to salt deposition and viscosity-induced changes in aerosolization efficiency in the nebulizer even though concentrations of REEs and internal standards were maintained constant. REE signal intensities were reduced by 25–35% in the final digestate (2% HNO_3) as compared to the aqueous solution. Additionally, similar suppression trends can be seen in Fig. 5 for ^{103}Rh, ^{115}In, and REEs suggesting that either would be appropriate for internal standardization. In contrast, ^{102}Ru and ^{185}Re exhibited a different trend compared with REEs demonstrating that they would not be effective internal standards for the FCC catalyst matrix. Hence, even though both ^{103}Rh and ^{115}In could be used, ^{115}In was chosen as the internal standard for REE quantitation in the catalyst digestate matrix using ICP-MS because its first ionization energy (558 kJ mol^{-1}) is within the range of all REEs (523–623 kJ mol^{-1}). Note that Rh has higher first ionization energy (720 kJ mol^{-1}).

3.5. Effect of HF amount

0, 0.05, 0.1, 0.3, 0.5 or 1.0 mL of HF was added to the first stage of microwave digestion to assess REE dissolution/extraction from FCC catalysts. Results from SMR1 and the spent catalyst are shown in Table 4. Method detection limits were also determined using the technique described in [31] and expressed in μg kg^{-1} of FCC catalyst. As observed, lighter REE (Y, La, Ce, Pr and Nd) concentrations increased most noticeably whereas Sm, Tb, Dy, Er and Yb increased moderately as HF volume increased from 0–0.05 to 0.1–0.3 mL. However, HF volumes >0.3 mL did not enhance dissolution of these REEs. In contrast, HF addition did not impact Eu, Gd, Ho, Tm and Lu concentrations. Similar results were obtained for other catalysts SMR2–SMR6.

These results demonstrate the need to employ HF to completely extract REEs from the aluminosilicate matrix of FCC catalysts. The acid mixture containing 5 mL HNO_3, 0.3 mL HF and 2.4 mL H_3BO_3 (method 4 in Table 4) necessitated a dilution factor of 3588 (mL per g sample) to achieve 2% HNO_3 in the final digestate prior to ICP analysis. Excessive HF did not enhance REE extraction but the concomitant H_3BO_3 addition increased total dissolved solids content deteriorating ICP-MS sensitivity. Hence, method 4 was chosen as the optimal digestion method, and employed in all future digestions. Moreover, quantitative recoveries of the two REEs (La, 98 ± 3% and Ce, 98 ± 2%) from a closely related catalyst (SRM 2556) lends further validity to using method 4 to extract REEs from FCC catalysts.

A Masuda–Coryell diagram (Fig. 6) was used to assess whether REE abundances in FCC catalysts were consistent with that found in nature [32] and to determine whether the zeolitic cation exchange processes by which catalysts were manufactured may have altered REE relative abundances in them. Catalysts REE concentrations were normalized by the corresponding weighted mean values in CI carbonaceous chondritic meteorites [33], because metals in these most primitive meteorites have not been chemically fractionated when relative abundances are compared with the photosphere. These meteorites apparently give us our most representative samples of the early solar system material, which was eventually incorporated into the earth. Natural samples will yield a smooth curve in a semi-logarithmic plot of chondrite normalized REE concentrations with respect to atomic number [16,17,32]. Exceptions for Ce and Eu can exist owing to their different oxidation states and redox geochemistry [34]. Chondrite normalized REE concentrations in FCC catalysts revealed several additional anomalies, including

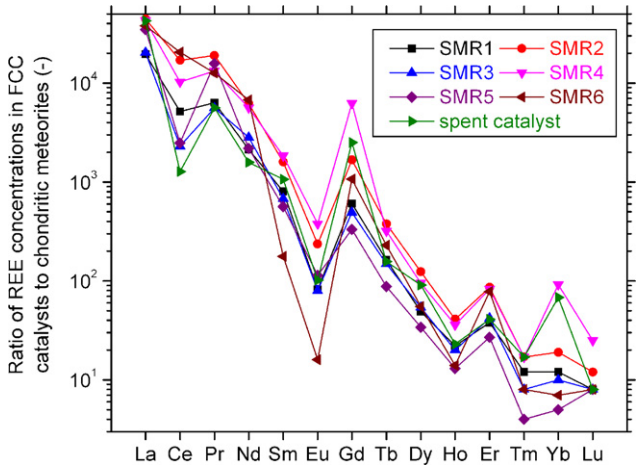

Fig. 6. Masuda–Coryell diagram or chondritic normalized plot suggesting alteration in REE composition in FCC catalysts compared to natural abundances. Chondritic meteorites concentrations obtained from [33].

Table 4
Influence of HF volume in the digestion mixture on REE concentrations analyzed by ICP-MS

REE	MDL, $\mu g\,kg^{-1}$	Method 1 (5 mL HNO_3)		Method 2 (5 mL HNO_3 + 0.05 mL HF + 0.4 mL H_3BO_3)		Method 3 (5 mL HNO_3 + 0.1 mL HF + 0.8 mL H_3BO_3)		Method 4 (5 mL HNO_3 + 0.3 mL HF + 2.4 mL H_3BO_3)		Method 5 (5 mL HNO_3 + 0.5 mL HF + 4.0 mL H_3BO_3)		Method 6 (5 mL HNO_3 + 1.0 mL HF + 8.0 mL H_3BO_3)	
		SMR1	Spent catalyst	SMR1	Spent catalyst	SMR1	Spent catalyst	SMR1	Spent catalyst	SMR1	Spent catalyst	SMR1	Spent catalyst
^{89}Y	2.982	16 ± 0.7	17.1 ± 1.1	33.7 ± 1.2	16.4 ± 1.3	20.5 ± 0.9	16.6 ± 0.6	22.0 ± 0.7	16.3 ± 0.8	22.3 ± 0.9	16.6 ± 0.8	22.1 ± 0.3	16.5 ± 0.6
^{139}La	5.471	3022 ± 34	4378 ± 88	3415 ± 41	5180 ± 58	4384 ± 53	8647 ± 111	4596 ± 40	10017 ± 77	4597 ± 49	9970 ± 81	4591 ± 56	9987 ± 73
^{140}Ce	3.524	1816 ± 24	714 ± 64	2778 ± 20	720 ± 62	2964 ± 34	737 ± 80	3122 ± 29	770 ± 66	3130 ± 26	787 ± 63	3128 ± 19	770 ± 79
^{141}Pr	4.792	467 ± 8	474 ± 25	545 ± 11	480 ± 18	541 ± 11	499 ± 22	568 ± 6	502 ± 27	566 ± 5	503 ± 13	567 ± 9	502 ± 11
^{146}Nd	6.082	647 ± 12	515 ± 20	888 ± 17	658 ± 12	926 ± 14	691 ± 21	943 ± 8	699 ± 26	945 ± 7	699 ± 15	969 ± 12	698 ± 16
^{147}Sm	3.169	117 ± 3	138 ± 7	121 ± 4	146 ± 4	116 ± 3	150 ± 6	114 ± 4	151 ± 6	122 ± 3	152 ± 8	123 ± 4	151 ± 4
^{153}Eu	2.310	4.4 ± 0.2	5.1 ± 0.3	4.5 ± 0.3	5.1 ± 0.2	4.4 ± 0.2	5.2 ± 0.2	4.1 ± 0.1	5.3 ± 0.2	4.6 ± 0.3	5.4 ± 0.2	4.5 ± 0.4	5.4 ± 0.2
^{157}Gd	4.175	105 ± 6	475 ± 6	102 ± 9	475 ± 4	100 ± 4	490 ± 8	106 ± 4	488 ± 11	108 ± 3	489 ± 9	106 ± 5	489 ± 5
^{159}Tb	1.318	2.2 ± 0.1	2.9 ± 0.1	3.0 ± 0.0	3.9 ± 0.1	3.2 ± 0.1	3.9 ± 0.1	3.6 ± 0.6	4.0 ± 0.2	4.0 ± 0.4	4.3 ± 0.1	3.9 ± 0.2	4.1 ± 0.2
^{163}Dy	2.993	8.8 ± 0.3	11 ± 0.6	8.8 ± 0.2	19.1 ± 1.1	11.4 ± 0.7	19.4 ± 0.9	12.3 ± 0.1	21.1 ± 1.6	12 ± 0.2	22.5 ± 1.4	12.6 ± 0.5	22.3 ± 1.0
^{165}Ho	0.273	1.0 ± 0.0	1.0 ± 0.1	0.8 ± 0.1	1.0 ± 0.0	1.0 ± 0.0	1.0 ± 0.0	1.1 ± 0.1	1.3 ± 0.0	1.2 ± 0.1	1.4 ± 0.1	1.1 ± 0.1	1.4 ± 0.0
^{166}Er	1.732	3.8 ± 0.2	4.2 ± 0.5	3.7 ± 0.2	4.0 ± 0.3	4.7 ± 0.3	4.2 ± 0.3	5.3 ± 0.5	6.2 ± 0.4	5.7 ± 0.4	6.4 ± 0.1	5.5 ± 0.4	6.3 ± 0.6
^{169}Tm	0.647	0.2 ± 0	0.2 ± 0	0.2 ± 0	0.4 ± 0	0.2 ± 0.0	0.3 ± 0	0.3 ± 0.0	0.4 ± 0.0	0.3 ± 0.0	0.4 ± 0.0	0.3 ± 0.0	0.4 ± 0.0
^{172}Yb	1.397	1.2 ± 0.1	1.9 ± 0.1	1.8 ± 0.1	2.6 ± 0.09	1.8 ± 0.1	2.4 ± 0.1	1.3 ± 0.2	7.1 ± 0.2	1.4 ± 0.1	8.2 ± 0.7	1.4 ± 0.2	6.6 ± 0.5
^{175}Lu	0.812	0.1 ± 0.0	0.2 ± 0.0	0.2 ± 0.0	0.2 ± 0.0	0.2 ± 0.0	0.2 ± 0.0	0.2 ± 0.0	0.2 ± 0.0	0.2 ± 0.0	0.2 ± 0.0	0.2 ± 0.0	0.2 ± 0.0

In all cases a two stage digestion was performed with set points of 200 °C and 200 psig with 20 min dwell time using 65% HNO_3, 48% HF and 5% H_3BO_3. Method detection limits were calculated as three times the standard deviation of seven analyses of a digested reagent blank solution employed as in method 4 spiked with REEs of interest each at half the lowest concentration used to calibrate the ICP-MS instrument as suggested in [31]. Results for one fresh FCC catalyst (SMR1) and one spent catalyst are shown. All concentrations (average ± standard deviation) are in $mg\,kg^{-1}$ except method detection limits (MDLs), which are in $\mu g\,kg^{-1}$.

Table 5
Non-REE elemental composition of FCC catalysts

Isotope	Fresh catalyst concentration range (mg kg^{-1})	Spent catalyst (mg kg^{-1})
^{23}Na	1208–4935	4240 ± 278
^{24}Mg	164–278	509 ± 5
^{27}Al	114,000–289,000	245,000 ± 8180
^{28}Si	221,000–268,000	200,000 ± 30,200
^{39}K	6336–23,287	20,600 ± 2100
^{45}Sc	19–28	37 ± 2
^{47}Ti	3819–9019	9109 ± 674
^{51}V	35–72	445 ± 5
^{52}Cr	52–124	133 ± 23
^{55}Mn	9.1–22.1	27.0 ± 0.4
^{57}Fe	2737–4838	5984 ± 63
^{59}Co	2.9–5.9	117 ± 2
^{60}Ni	12–24	1094 ± 12
^{63}Cu	7–23	46.5 ± 0.2
^{68}Zn	59–123	153 ± 2
^{69}Ga	35–71	63 ± 1
^{75}As	6.2–15.9	6.3 ± 0.0
^{77}Se	14.9–56.3	28.6 ± 0.1
^{85}Rb	2–4	2.5 ± 0.0
^{88}Sr	35–105	53.0 ± 1.1
^{90}Zr	47–78	66.3 ± 0.4
^{95}Mo	1.1–2.2	12.2 ± 0.1
^{111}Cd	<MDL (=0.5)	<MDL (=0.5)
^{133}Cs	0.24–0.27	0.22 ± 0.06
^{137}Ba	85–255	134.1 ± 2.1
^{208}Pb	22–45	48 ± 1
^{238}U	1.6–3.9	2.8 ± 0.1

All concentrations are in mg kg^{-1}.

Gd, Er and Yb indicating substantial anthropogenic alterations (see Fig. 6). These anomalies demonstrate changes in natural REE abundances in FCC catalysis probably arising during the stripping of REE cations in the zeolite matrix [35]. Unusual anomalies for Gd, Er and Yb distinguish the matrix of FCC catalysts from previously investigated samples such as peat, plant, soil, sediment, tissue, etc., that preserve natural REE abundances necessitating this research.

Table 5 compares concentrations of non-REEs in six fresh catalysts and the spent catalyst obtained using the newly developed method. As expected from the aluminosilicate backbone of zeolitic catalysts employed in this study, Al and Si were most dominant together accounting for 36–54% of the mass. K, Na and Ti were also present in very high levels collectively constituting 1.4–3.4% of the measured mass. Concentrations of Ni, V, Co, Cu and Mo were substantially increased (∼2–50-fold) in the spent catalyst compared with fresh catalysts demonstrating poisoning. Chemical contamination by these metals beyond the range of fresh catalysts coupled with morphological changes (Fig. 1) not only reduces catalytic activity during refining, but validates our choice of including a spent catalyst for method development research reported herein.

3.6. Predigestion matrix spike recoveries

Table 6 shows REE spike recoveries from all seven FCC catalysts and the zeolite powder along with the amount of spike

Table 6
REE spike recoveries (%) from aged FCC catalysts and zeolite

Analyte	Concentration range in all seven FCC catalysts (mg kg^{-1})	Spike added (ng)	SMR1 (%)	SMR2 (%)	SMR3 (%)	SMR4 (%)	SMR5 (%)	SMR6 (%)	Spent catalyst (%)	Zeolite (%)
^{89}Y	10.6–43.1	100	109 ± 5	113 ± 4.7	102 ± 4	112 ± 4	89 ± 6	98 ± 5	109 ± 6	98 ± 3
^{139}La	4597–10,452	40,000	96 ± 6	108 ± 4.7	112 ± 3	113 ± 4	110 ± 5	109 ± 4	112 ± 3	102 ± 4
^{140}Ce	770–12378	40,000	88 ± 8	101 ± 4.8	103 ± 5	94 ± 3	95 ± 6	96 ± 4	92 ± 7	98 ± 6
^{141}Pr	499–1696	5,000	93 ± 4	95 ± 4.6	92 ± 6	93 ± 9	90 ± 4	90 ± 10	95 ± 4	95 ± 3
^{144}Nd	716–3054	10,000	108 ± 4	100 ± 9.2	105 ± 7	107 ± 7	111 ± 5	112 ± 3	92 ± 2	95 ± 1
^{152}Sm	26–271	700	99 ± 1	101 ± 8.0	102 ± 11	103 ± 3	105 ± 4	100 ± 4	104 ± 9	104 ± 3
^{153}Eu	0.9–21.1	40	97 ± 2	100 ± 5.2	103 ± 6	104 ± 2	98 ± 8	103 ± 5	106 ± 3	102 ± 6
^{157}Gd	65–1228	2,000	110 ± 5	101 ± 4.4	98 ± 4	108 ± 5	112 ± 4	111 ± 4	117 ± 1	98 ± 4
^{159}Tb	3.2–13.7	40	106 ± 5	86 ± 0.9	104 ± 2	89 ± 2	85 ± 4	88 ± 1	107 ± 2	103 ± 2
^{162}Dy	8.2–30.0	100	102 ± 7	111 ± 5.3	114 ± 10	97 ± 10	93 ± 6	107 ± 1	94 ± 1	103 ± 4
^{165}Ho	0.7–2.3	5	105 ± 3	106 ± 8.4	112 ± 13	109 ± 27	107 ± 3	108 ± 9	107 ± 8	98 ± 1
^{166}Er	4.3–13.7	50	105 ± 4	99 ± 8.1	90 ± 10	93 ± 11	106 ± 5	109 ± 4	87 ± 4	102 ± 1
^{169}Tm	0.1–0.4	5	110 ± 5	93 ± 5.6	89 ± 6	90 ± 5	108 ± 5	103 ± 12	89 ± 6	100 ± 2
^{172}Yb	0.8–14.9	25	92 ± 3	90 ± 4.6	112 ± 4	106 ± 5	109 ± 5	108 ± 5	105 ± 3	102 ± 1
^{175}Lu	0.2–0.6	5	92 ± 3	85 ± 6.0	94 ± 3	97 ± 4	113 ± 6	94 ± 10	91 ± 4	95 ± 3

Spikes were added 90 days before microwave digestion with $HNO_3 + HF + H_3BO_3$. For each REE, average spike recovery and standard deviation of 3–6 measurements are reported.

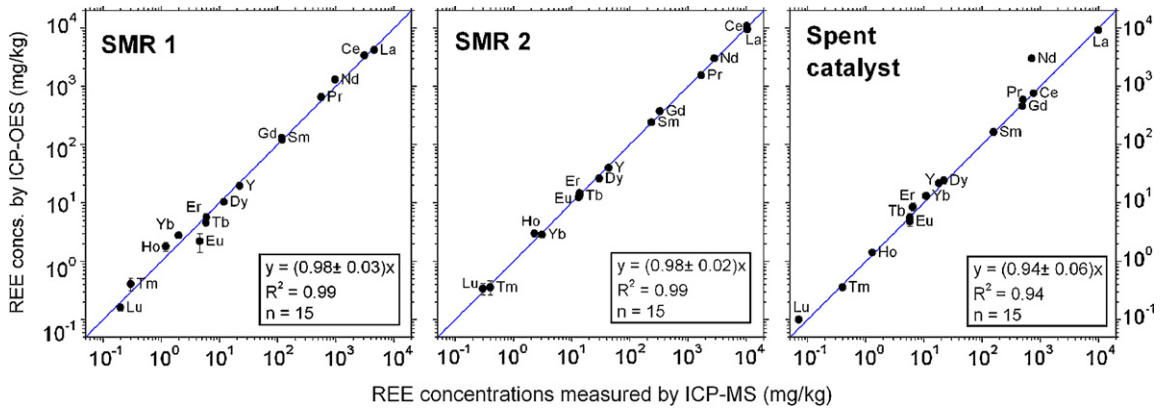

Fig. 7. Scatter plots of REE concentrations in FCC catalysts measured using ICP-MS and ICP-OES. The solid line denotes perfect equality between the two measurement techniques.

added to each sample. Excellent recoveries with <15% error confirm the applicability of digestion method 4 to extract REEs from the solid catalyst samples.

3.7. Comparison of ICP-MS and ICP-OES

All FCC catalyst samples were digested using the optimal method and also analyzed by ICP-OES. Typical results obtained are depicted in Fig. 7 in the form of a bivariate scatter plot. Excellent agreement between ICP-MS and ICP-OES measurements of REEs can be observed in two fresh catalysts (SMR1 and SMR2) and the spent catalyst. Similar results were obtained for SMR3–SMR6. Paired *t*-tests and regression analysis revealed no statistical differences between the two methods at 95% confidence for all catalyst samples. Hence, REE analyses of the digestate using ICP-MS were accurate and precise. Note that using ICP-OES only allows the verification of our ICP-MS results. Because ICP-OES and ICP-MS were performed on the same sample digestate, this comparison does not validate the digestion methodology.

3.8. Comparison of ICP-MS and INAA

Using the INAA represents a more stringent validation of the newly developed method because it does not require sample digestion. To evaluate both sample digestion and ICP-MS analysis of the newly developed method (method 4 in Table 4), direct REE measurements from solid samples were performed using INAA.

Table 7 summarizes quantitative deviation between ICP-MS and INAA in all catalysts in terms of relative percent deviation (RPD) [37,38] calculated as:

$$\text{RPD}\,(\%) = \frac{|X_{\text{ICP-MS}} - X_{\text{INAA}}|}{1/2(X_{\text{ICP-MS}} + X_{\text{INAA}})} \times 100$$

where X is the element chosen for comparison. As depicted in Table 7, 62 of 81 results (77%) agreed within 20% RPD. Similar to previous reports of REE analyses from peat, plant, rock and rice, higher RPDs (>20%) were typically observed for Tb, Yb and Lu [16,36]. As explained in Section 3.3, large corrections (15–45%) for spectral overlap were made for these elements during ICP-MS analysis, potentially contributing to the observed discrepancy with INAA. Hence, care should be taken prior to report Tb, Yb and Lu from several matrices. Further, as observed from Fig. 8, ICP-MS and INAA agreed very closely (except for La in spent catalyst). Results summarized in Fig. 8 and Table 7 demonstrates that INAA results agreed well with ICP-MS measurements for most REEs and substantiate the newly developed method. Hence, for FCC catalysts, ICP-MS maybe better suited than INAA for Pr, Gd, Dy, Ho, Er and Tm, both ICP-MS and

Table 7
Inter-comparison of ICP-MS and INAA measurements in terms of relative percentage deviation

	SMR1	SMR2	SMR3	SMR4	SMR5	SMR6	Spent
Na	8	39	14	54	58	19	17
Fe	12	16	11	13	10	23	1
Co	7	8	4	4	0	7	5
Ba	10	1	4	4	Not analyzed by INAA	Not analyzed by INAA	Not analyzed by INAA
La	11	15	9	8	2	4	72
Ce	9	15	8	8	2	12	82
Nd	10	20	13	15	15	13	12
Sm	3	13	8	2	4	9	1
Eu	8	25	6	14	1	8	5
Tb	31	40	35	37	19	95	34
Yb	12	3	18	79	35	35	115
Lu	10	28	15	39	2	3	17

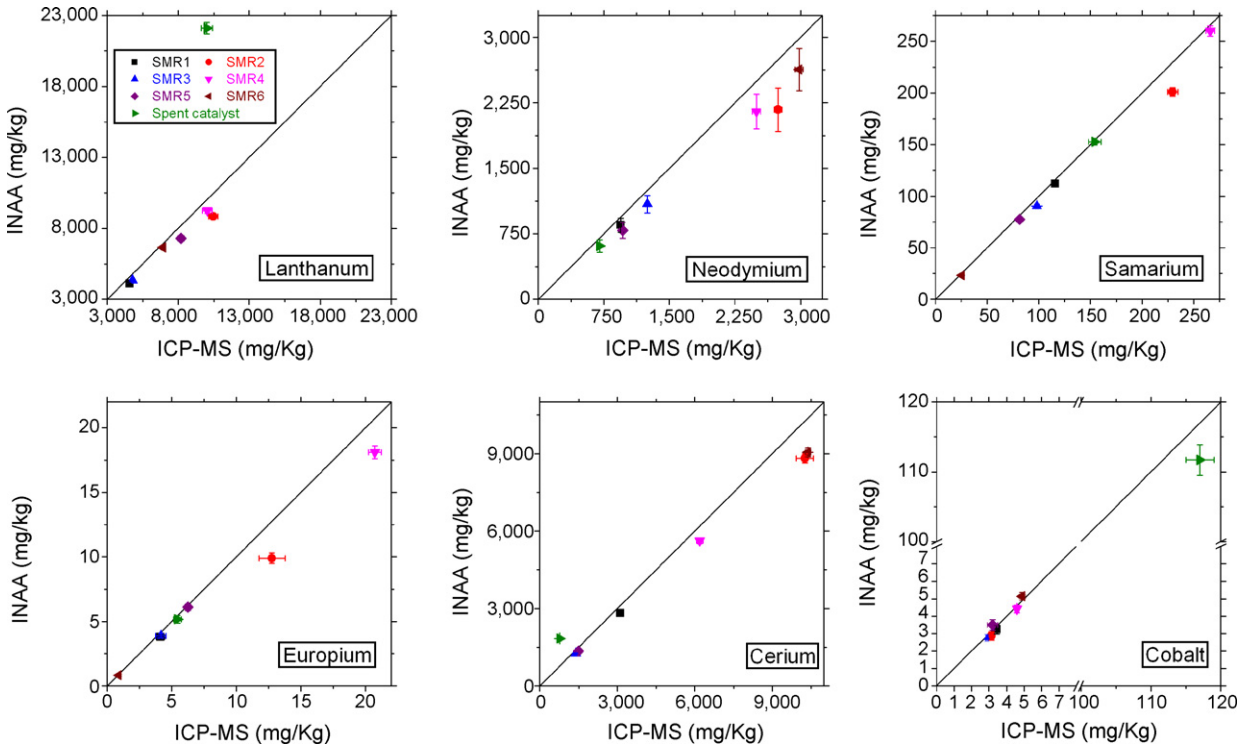

Fig. 8. Scatter plots of La, Ce, Nd, Sm, Eu and Co concentrations in seven FCC catalysts measured using ICP-MS and INAA. Light REEs were chosen for graphical comparison because they are more abundant than heavy REEs. The solid line denotes perfect equality between the two measurement techniques.

INAA are capable of accurately analyzing La, Ce, Nd, Sm and Eu, whereas INAA maybe better suited than ICP-MS for Tb, Yb and Lu.

3.9. Analysis of ambient fine particulate matter

The optimal digestion technique (method 4 in Table 4) was also used to extract REEs from atmospheric $PM_{2.5}$ samples prior to ICP-MS analysis. HF and H_3BO_3 volumes were reduced proportionately to digest the lower PM mass collected on each filter (0.2–0.5 mg) compared to the 50 mg FCC catalyst mass employed for method development (see Section 3.5). A minimum 3 mL HNO_3 was necessary to monitor temperature profiles within the digestion vessels employed (HP500 plus) and to prevent potential localized overheating of the liners.

Using this procedure, eight REEs (La, Ce, Pr, Nd, Sm, Eu, Gd and Dy) were detected in $PM_{2.5}$ samples from Houston's Ship Channel area, which are depicted in Fig. 9 in the form of a time series. Matrix spike recoveries of each of these elements were in the range 84–108% indicating accurate analysis. Enrichment of these REEs in $PM_{2.5}$ has already been quantitatively traced back to catalyst emissions from petroleum refining operations [10,12]. Further, Fig. 9 depicts that La, Ce, Pr, Nd, Sm, Gd and Dy profiles were in phase, following each other very closely, and even peaking on the same days (3 June and 14 August). Statistically significant and positive correlations ($p = 0.01$) were also observed between each of these REEs signifying a common emission source (FCC catalysts). In contrast, because Eu concentrations in FCC catalysts and local soil were in the same range [10], its profile was not in phase with other REEs as it was emitted by at least these two sources. Further, as seen in Fig. 9, the digestion and analysis method developed herein successfully captured three orders of magnitude variation in REEs (e.g. Dy in pg m^{-3} and La in ng m^{-3}) demonstrating its suitability to analyze trace to ultra-trace REEs levels in $PM_{2.5}$.

3.10. REEs as markers of FCC catalysts emissions

Source apportionment calculations have demonstrated that REEs in $PM_{2.5}$ predominantly originate from FCC operations

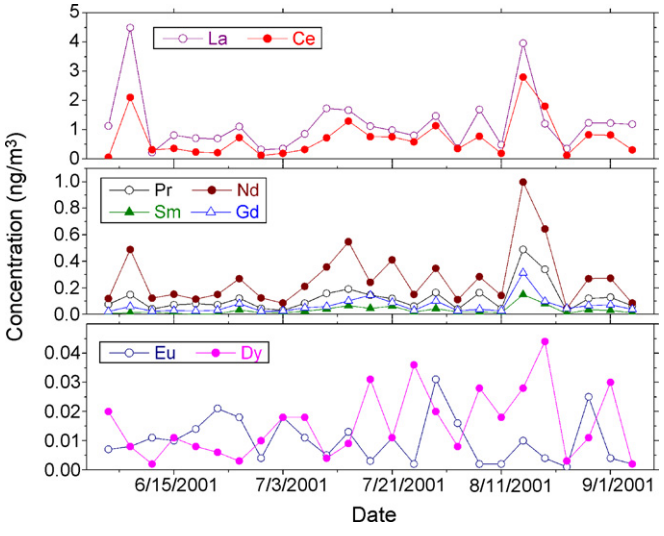

Fig. 9. REE concentrations in 25 $PM_{2.5}$ samples collected in Houston's Ship Channel area.

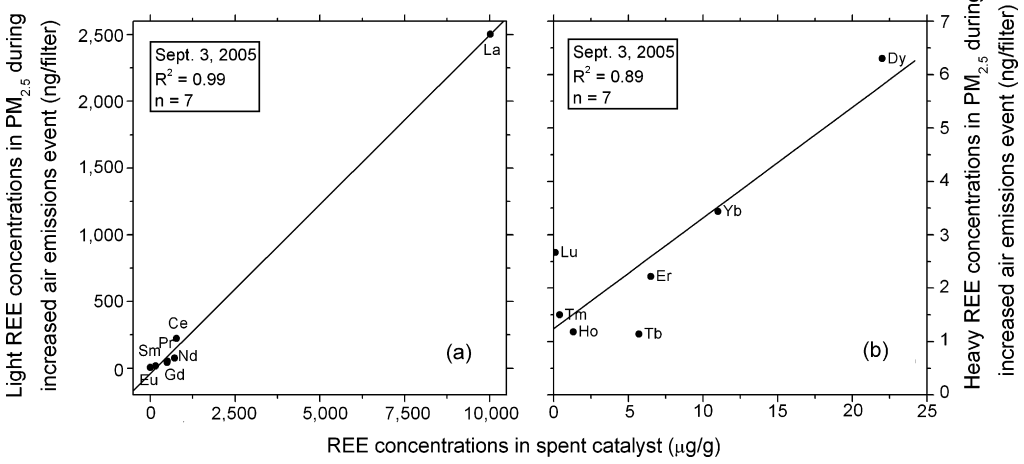

Fig. 10. Comparison of REE concentrations in ambient $PM_{2.5}$ spent FCC catalyst.

[10]. Additional data linking malfunctions in petroleum refineries to increased REEs in atmospheric fine particles are shown herein. Fig. 10 compares REE concentrations measured during the increased air emissions event on 03 September 2005 and the spent catalyst. Enrichment factors were also calculated for each REE using Nd as the reference because it was present in ~100-fold higher concentrations in the spent catalyst compared to the local soil [10]:

$$\text{Enrichment factor}\,(X) = \frac{[X]_{PM_{2.5}}/[Nd]_{PM_{2.5}}}{[X]_{\text{spent catalyst}}/[Nd]_{\text{spent catalyst}}}$$

Strong positive correlations were observed for light REEs, viz. La, Ce, Nd, Pr, Gd, Sm and Eu in Fig. 10a ($R^2 = 0.99$) and for heavy REEs, viz. Tb, Dy, Ho, Er, Tm, Yb and Lu in Fig. 10b ($R^2 = 0.89$). Enrichment factors for all REEs (except Ho, Tm and Lu) were all close to unity indicating that FCC catalysts were also emitted to the local atmosphere during the increased air emissions event. Enrichment of Ho, Tm and Lu in $PM_{2.5}$ can be attributed to their higher concentrations in local soil compared with catalysts [10]. Similar to our recent observations of background REE levels in the Houston atmosphere [10], the REE abundance sequence in the spent catalyst and the $PM_{2.5}$ sample during the increased air emissions event were similar (La > Ce > Nd > Pr > Gd > Sm > Dy > Eu ~ Er ~ Yb ~ Lu ~ Tb ~ Ho). Finally, the ratio of La and Ce, which were the two dominant REEs in the spent catalyst and $PM_{2.5}$ during the emission event were very similar (11.2 and 13.0, respectively). Hence, the increase in $PM_{2.5}$ mass during the increased air emissions event in the refinery was predominantly caused by the loss of FCC catalyst.

4. Summary and conclusions

Closed vessel microwave acid digestion with set points at 200 °C, 200 psig, and 20 min dwell time using 5 mL HNO_3 (65%), 0.3 mL HF (48%) and 2.4 mL H_3BO_3 (5%, m/v) quantitatively extracted 15 REEs and 27 other elements from 50 mg of FCC catalysts. The same digestion method with reduced acid volumes (3 mL HNO_3, 3 μL HF and 24 μL H_3BO_3) could also identify eight REEs (La, Ce, Pr, Nd, Sm, Eu, Gd and Dy) in ambient atmospheric fine particles. Results reported herein are valuable to on-going efforts at the National Institute of Standards and Technology to develop a FCC catalyst standard reference material [15]. Additionally, analyzing REEs would enhance air quality monitoring studies by providing clues to the origin of ambient aerosols in daily ambient $PM_{2.5}$ samples [10] as well as increased $PM_{2.5}$ concentrations caused by breakdowns of pollution control equipment in refineries. Hence, REEs analysis is recommended for quantitative apportionment of petroleum refining operations to $PM_{2.5}$ mass in industrialized environments.

Acknowledgments

This project has been supported with funds from the State of Texas as part of the program of the Texas Air Research Center. The JSC INAA facility is funded by a grant from the NASA Cosmochemistry Program to DWM. We thank John Hernandez and the personnel of the Nuclear Science Center of Texas A&M University for their capable handling of the neutron irradiation. The contents do not necessarily reflect the views and policies of the sponsor nor does the mention of trade names or commercial products constitute endorsement or recommendation for use. We also thank Karl Loos of Shell, Tom Habib and Larry McDorman of Grace Davison, Wei Wang of the City of Houston, and Matt Fraser of Rice University for providing samples.

References

[1] J.G. Watson, T. Zhu, J.C. Chow, J. Engelbrecht, E.M. Fujita, W.E. Wilson, Chemosphere 49 (2002) 1093.
[2] An introduction to source receptor modeling, in: P.K. Hopke in, S. Landsberger, M. Creatchman (Eds.), Elemental Analysis of Airborne Particles, Gordan and Breach Science Publisher, Amsterdam, The Netherlands, 1999, p. 273 (chapter 8).
[3] A.M. Dillner, J.J. Schauer, W.F. Christensen, G.R. Cass, Atmos. Environ. 39 (2005) 1525.
[4] P. Kulkarni, S. Chellam, G. Ghurye, M.P. Fraser, Environ. Eng. Sci. 20 (2003) 517.
[5] N.J. Pekney, C.I. Davidson, Anal. Chim. Acta 540 (2005) 269.

[6] J.C. Chow, J.G. Watson, H. Kuhns, V. Etyemezian, D.H. Lowenthal, D. Crow, S.D. Kohl, J.P. Engelbrecht, M.C. Green, Chemosphere 54 (2004) 185.
[7] K. Swami, C.D. Judd, J. Orsini, K.X. Yang, L. Husain, Fresen. J. Anal. Chem. 369 (2001) 63.
[8] J.D. Herner, P.G. Green, M.J. Kleeman, Environ. Sci. Technol. 40 (2006) 1925.
[9] I. Olmez, G.E. Gordon, Science 229 (1985) 966.
[10] P. Kulkarni, S. Chellam, M.P. Fraser, Atmos. Environ. 40 (2006) 508.
[11] F.A. Cotton, G. Wilkinson, C.A. Murillo, M. Bochmann, Advanced Inorganic Chemistry, Wiley, New York, 1999.
[12] M.E. Kitto, D.L. Anderson, G.E. Gordon, I. Olmez, Environ. Sci. Technol. 26 (1992) 1368.
[13] G.C. Lough, J.J. Schauer, J.-S. Park, M.M. Shafer, J.T. Deminter, J.P. Weinstein, Environ. Sci. Technol. 39 (2005) 826.
[14] J.A. Sternbeck, A. Sjodin, K. Andreasson, Atmos. Environ. 36 (2002) 4735.
[15] R. Zeisler, Research Chemist Analytical Chemistry Division, National Institute of Standards and Technology (NIST), Gaithersburg, MD, 2005, personal communication.
[16] M. Krachler, C. Mohl, H. Emons, W. Shotyk, J. Anal. Atom. Spectrom. 17 (2002) 844.
[17] T. Prohaska, S. Hann, C. Latkoczy, G. Stingeder, J. Anal. Atom. Spectrom. 14 (1999) 1.
[18] T.P. Rao, V.M. Biju, Crit. Rev. Anal. Chem. 30 (2000) 179.
[19] V. Balaram, J. Appl. Geochem. 4 (2B) (2002) 493.
[20] M.I. Rucandio, Anal. Chim. Acta 264 (1992) 333.
[21] K. Shinotsuka, M. Ebihara, Anal. Chim. Acta 338 (1997) 237.
[22] N.M.P. Moraes, S.S. Iyer, Anal. Chim. Acta 236 (1990) 487.
[23] J. Riondato, F. Vanhaecke, L. Moens, R. Dams, Fresen. J. Anal. Chem. 370 (2001) 544.
[24] B. Buzcu, M.P. Fraser, P. Kulkarni, S. Chellam, Environ. Eng. Sci. 20 (2003) 533.
[25] M.L. Occelli, P. O'Connor (Eds.), Fluid Cracking Catalysts. V. Materials and Technological Innovations, in: B. Delmon, J.T. Yates (Eds.), Studies in Surface Science and Catalysis, vol. 134, Elsevier Science B.V., New York NY, 1998.
[26] M.B. Shabani, T. Akagi, S. Hiroshi, A. Masuda, Anal. Chem. (1990) 2709.
[27] J. Aggarwal, M. Shabani, M. Psalmer, K. Rangnarsdottir, Anal. Chem. 68 (1996) 4418.
[28] D.J. Lindstorm, R.L. Korotev, J. Radioanal. Chem. 70 (1982) 439.
[29] H.M. Kingston, L.B. Jassie (Eds.), Microwave Enhanced Chemistry, ACS Professional Reference Series, Washington, DC, 1997.
[30] P. Dulski, Fresen. J. Anal. Chem. 350 (1994) 194.
[31] L.S. Clesceri, A.E. Greenberg, A.D. Eaton (Eds.), Standard Methods for the Examination of Water and Wastewater, 20th ed., American Public Health Association/American Water Works Association/Water Environment Federation, Washington, DC, 1998.
[32] P. Henderson, Inorganic Geochemistry, Pergamon Press, New York, 1982.
[33] K. Lodders, Astrophys. J. 591 (2003) 1220.
[34] C.P. Marshall, R.W. Fairbridge, Encyclopedia of Geochemistry, Kluwer Academic Publishers, Dordrecht, The Netherlands, 1999.
[35] J.T. Richardson, Principles of Catalyst Development, Plenum Press, New York, 1989.
[36] M.P. Huynh, F. Carrot, S.C.P. Ngoc, M.D. Vu, G. Revel, J. Radioanal. Nucl. Chem. 217 (1997) 95.
[37] D.L. Massart, B.G.M. Vandeginste, L.M.C. Buydens, S. De Jong, P.J. Lewi, J. Smeyers-Verbeke, Handbook of Chemometrics and Qualimetrics. Part A. Data Handling in Science and Technology, vol. 20A, Elsevier Science, Amsterdam, The Netherlands, 1997.
[38] C.F. Wang, E.E. Chang, P.C. Chiang, N.K. Aras, Analyst 120 (1995) 2521.